



Multiple cystic sphere formation from PK-8 cells in three-dimensional culture

Yuuki Shichi^a, Fujiya Gomi^a, Yoshibumi Ueda^b, Keisuke Nonaka^a, Fumio Hasegawa^a, Yasuko Hasegawa^a, Nae Hinata^c, Hisashi Yoshimura^d, Masami Yamamoto^d, Kimimasa Takahashi^e, Tomio Arai^f, Toshiyuki Ishiwata^{a,*}

^a Division of Aging and Carcinogenesis, Research Team for Geriatric Pathology, Tokyo Metropolitan Institute of Gerontology, Tokyo, 173-0015, Japan

^b Department of Chemistry, School of Science, The University of Tokyo, Tokyo, 113-8654, Japan

^c Department of Clinical Engineering School of Health Sciences, Tokyo University of Technology, Tokyo, 144-8535, Japan

^d Laboratory of Physiological Pathology, Department of Applied Science, School of Veterinary Nursing and Technology, Nippon Veterinary and Life Science University, Tokyo, 180-8602, Japan

^e Department of Veterinary Pathology, School of Veterinary Medicine, Nippon Veterinary and Life Science University, Tokyo, 180-8602, Japan

^f Department of Pathology, Tokyo Metropolitan Geriatric Hospital and Institute of Gerontology, Tokyo, 173-0015, Japan

ARTICLE INFO

Keywords:

Pancreatic ductal adenocarcinoma/PDAC
E-cadherin
PK-8
Sphere
Cyst
Three-dimensional culture

ABSTRACT

Three-dimensional (3D) culture of cancer cells mimics the *in vivo* environment. Recently, we reported that pancreatic ductal adenocarcinoma (PDAC) cell lines with epithelial and mesenchymal features formed differently shaped spheres in 3D culture. However, only PK-8 cells, the epithelial PDAC cell line with the highest *E-cadherin* expression among the eight PDAC cell lines, formed multiple cystic spheres in 3D culture. Optical coherence tomography revealed interconnected cysts inside the spheres. A weak inter-cellular adhesion, individual cell degeneration, necrosis, and secretory granules in the cytoplasm were observed in the PK-8 spheres using electron microscopy. The expression of MUC1, MUC5AC, and amylase was increased in PK-8 cells in the 3D culture compared with that in 2D culture. These findings suggest that highly *E-cadherin*-expressing epithelial PK-8 cells form multiple cystic spheres, which may be promoted by enhanced mucin and amylase synthesis in 3D culture.

1. Introduction

Pancreatic ductal adenocarcinoma (PDAC), a major form of pancreatic cancer, is one of the most lethal tumors. In the Western world, the 5-year survival rate of PDAC is only 9% [1]. Most (80–90%) patients with PDAC are not eligible for radical surgery due to local recurrence or metastasis at diagnosis. Even patients with PDAC who can be operated on relapse or metastasize after surgery, and the 5-year survival rate is only 15–20% [2]. Age is a major risk factor for cancer [3], and an increase in pancreatic cancer-related deaths is expected because of the rapidly aging population in developed countries. Pancreatic cancer is expected to be the second leading cause of cancer-related deaths, and the first among digestive cancers worldwide by 2030 [4].

To date, approximately 400 human PDAC cell lines have been reported, and studies using two-dimensional (2D) culture methods have traditionally been carried out [5]. However, three-dimensional (3D) cell

culture methods are considered to mimic the *in vivo* environment because both primary and metastatic tumors form 3D masses [6,7]. Transcriptional analyses of PDAC cell lines have suggested two molecular subtypes, the classical and quasi-mesenchymal cell lines [8]. The classical subtype is characterized by the expression of epithelial and adhesion-related genes, whereas the quasi-mesenchymal subtype expresses mesenchymal genes. Patients with PDAC with the classical subtype have a better prognosis, whereas the prognosis of the quasi-mesenchymal subtype is worse [8]. Using 3D culture, we found that PDAC cell lines with high *E-cadherin* and low vimentin levels (epithelial) formed small, round spheres encased in flat, lining cells, whereas those with the alternate expression pattern (mesenchymal) formed large, grape-like spheres without the perimeter cells [5,9,10]. Furthermore, gemcitabine was more effective on epithelial PDAC spheres, while nab-paclitaxel was effective on mesenchymal PDAC spheres [9]. Among the eight PDAC cell lines examined, PK-8 cells were epithelial-featured PDAC cell lines with the highest *E-cadherin* mRNA

* Corresponding author. 35-2 Sakae-cho, Itabashi-ku, Tokyo, 1C73-0015, Japan.

E-mail address: tishiwat@tmig.or.jp (T. Ishiwata).

<https://doi.org/10.1016/j.bbrep.2022.101339>

Received 12 July 2022; Received in revised form 15 August 2022; Accepted 30 August 2022

2405-5808/© 2022 The Authors. Published by Elsevier B.V. This is an open access article under the CC BY-NC-ND license (<http://creativecommons.org/licenses/by-nc-nd/4.0/>).

expression and were the only cell line with a large number of hole-like structures in the spheres under 3D culture. PDAC is pathologically characterized by ductal formation at variable levels in human tissues, and transforming growth factor- β signaling has been reported to promote tube-forming growth in PDAC cell lines [11]. Normal parenchymal pancreatic cells have the potential to synthesize and secrete exocrine and endocrine molecules and mucins. On the other hand, most PDAC cells synthesize mucins, but do not synthesize and secrete exocrine and endocrine molecules.

In this study, we investigated the morphological and functional features of the hole-like structures formed by PK-8 spheres and identified increased expression of exocrine molecules and mucins, and the formation of multiple cystic (but not ductal) structures in the spheres.

2. Materials and methods

2.1. Cell culture

Human PDAC cell line PK-8 was provided by the RIKEN BioResource Research Center through the National Bio-Resource Project of the Ministry of Education, Culture, Sports, Science and Technology, Japan. Cells were grown in RPMI 1640 medium containing 10% fetal bovine serum at 37 °C in a humidified 5% CO₂ atmosphere. To form spheres, cells (3×10^3 cells/well) were seeded in 96-well ultra-low attachment plates (Thermo Fisher Scientific, Waltham, MA, USA) [9]. After seven days, the spheres were photographed using a phase-contrast microscope (Eclipse TS-100, Nikon, Tokyo, Japan). The spheres were then aspirated using micropipettes and used in further experiments.

2.2. Scanning electron microscopy (SEM)

Adherent PK-8 cells were fixed for 30 min, and PK-8 spheres were fixed overnight with 2.5% glutaraldehyde in 0.1 M phosphate buffer (pH 7.4) at 4 °C. The glutaraldehyde solution was then removed, and the cells were washed with phosphate-buffered saline. The PK-8 cells were post-fixed with OsO₄ for 30 min. After complete dehydration via a graded ethanol series, the samples were suspended in 100% ethanol, air-dried, and coated with a platinum layer using an MSP-1S sputter coater (Shinku Device, Ibaraki, Japan) [12]. Cells were examined and photographed using a Phenom Pro desktop scanning electron microscope using secondary electrons and reflected electrons for the attached cells and spheres, respectively (Thermo Fisher Scientific).

2.3. Immunocytochemical analysis

Cell blocks were prepared as previously reported, with minor modification [9,10]. The spheres were collected using a micropipette under a microscope, and adherent cells were detached using trypsin and fixed in 10% neutral-buffered formalin for 3 h. Formalin was removed using a micropipette, dehydrated with graded ethanol, and embedded in paraffin. Serial sections of the cell blocks (4- μ m thickness) were either stained with hematoxylin and eosin (H&E) or immunostained using the labeled streptavidin-biotin method. The following primary antibodies were used for immunocytochemical staining: mouse monoclonal anti-E-cadherin (M106, Takara Bio, Shiga, Japan), mouse monoclonal anti-vimentin (422101, Nichirei Biosciences Inc., Tokyo, Japan), mouse monoclonal anti-MUC1 (NCL-MUC-1, Leica Biosystems, Wetzlar, Germany), mouse monoclonal anti-MUC5AC (NCL-MUC-5AC, Leica Biosystems, Wetzlar, Germany), and mouse monoclonal anti-amylase alpha (Proteintech Group, Inc., Rosemont, IL, USA). The sections were treated with 0.03% H₂O₂ in 33% methanol at room temperature for 30 min to block endogenous peroxidase before antigen retrieval. The reaction to each antigen was visualized by adding 3,3'-diaminobenzidine tetrahydrochloride (DAB) and counterstaining with hematoxylin. Negative controls were generated by omitting the primary antibodies. Images were taken using an upright microscope (BX43; Olympus, Tokyo,

Japan). To measure cells positive for MUC1, MUC5AC, and amylase, images were captured by Mantra 2, multi-spectral microscopy (PhenoImager Mantra2, AKOYA Biosciences, Marlborough, MA, USA). The images were loaded into the inForm software ver.2.4 (AKOYA Biosciences) to count the positive cells with a 20 \times objective lens.

2.4. Optical coherence tomography (OCT) observation of the spheres

The spheres were collected using a micropipette under a microscope and fixed in 10% neutral buffered formalin. Unstained spheres were imaged by OCT using a Cell3iMager Estier (SCREEN Holdings Co., Ltd., Kyoto, Japan). The values for multiple parameters based on the Gardner classification were obtained from the 3D image data. The system was equipped with a superluminescent diode (SLD; center wavelength:890 nm, N.A. = 0.3). The SLD output was coupled to a single-mode optical fiber and split at an optical fiber coupler into sample and reference arms. Reflections from the two arms were combined at the coupler and detected using a spectrometer. The 3D image data of the spheres were constructed from individual 2D x-z cross-sectional images, which were obtained using a series of longitudinal scans by laterally translating the optical beam position. The data acquisition window was 200–300 \times 200–300 \times 200–300 μ m and the voxel size was 1 \times 1 \times 1 μ m.

2.5. Transmission electron microscopy (TEM)

TEM images were acquired as previously reported [13]. Spheres from PK-8 cells were fixed with 2.5% glutaraldehyde in 0.1 M phosphate buffer (pH 7.4), post-fixed for 1 h with 2% OsO₄ dissolved in distilled water, dehydrated in a graded series of ethanol solutions, and embedded in Epon. Ultrathin sections were generated and stained with uranyl acetate and lead citrate for observation under a transmission electron microscope (H-7500; Hitachi High-Technologies, Tokyo, Japan).

2.6. Quantitative reverse transcription-polymerase chain reaction (qRT-PCR)

Total RNA from PK-8 adhesive cells and spheres was isolated using the PureLink® RNA Mini Kit (Thermo Fisher Scientific K.K., Tokyo, Japan). Subsequently, 400 ng of RNA was reverse-transcribed using the PrimeScript™ II 1st strand cDNA Synthesis Kit (TAKARA BIO Inc., Shiga, Japan). qRT-PCR was performed with SYBR® Green Real-Time PCR Master Mix (Thermo Fisher Scientific K.K., Tokyo, Japan) using a Thermal Cycler Dice® Real Time System TP800 (TAKARA BIO Inc., Shiga, Japan). The $\Delta\Delta$ Ct method was used to analyze the data. ACTB was used as an internal control to normalize the expression of the target gene(s) between different samples. The primer sets used for qRT-PCR are listed in Table S1. All values are expressed as the mean \pm standard error of the mean (S.E.M.). Statistical analyses were performed using Student's *t*-test. Asterisks (*) were used to indicate P values < 0.05, and N.S. indicates no significant difference.

3. Results

3.1. High E-cadherin expression in PK-8 cells under 3D culture

Under the 2D-culture condition, PK-8 cells proliferated in a sheet form, and SEM showed a large number of microvilli between the PK-8 cells (Fig. 1, upper left panels). Immunocytochemically, E-cadherin positivity was detected in a small number of PK-8 cells (Fig. 1, arrows), whereas no vimentin signal was observed (Fig. 1, upper right panels). PK-8 cells cultured in 96-well ultra-low attachment plates formed irregularly shaped spheres with multiple translucent cysts of various sizes (Fig. 1, lower-left panels). SEM analysis showed that the surface of the sphere was flat and covered with adherent cancer cells, and large and small holes formed by ruptured cysts were observed. Immunocytochemical analysis revealed a strong E-cadherin expression on the

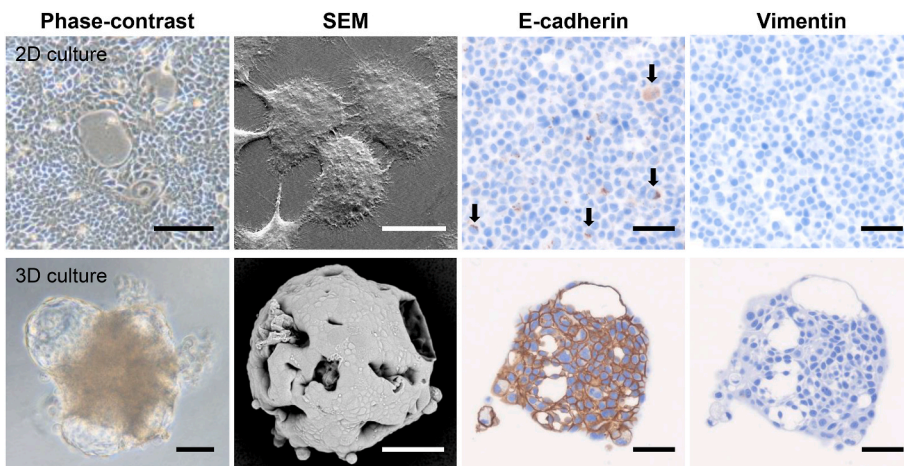


Fig. 1. Phase contrast and scanning electron microscopy (SEM) and immunocytochemical analyses of PK-8 cells under 2D and 3D culture conditions. Representative phase contrast and SEM images of PK-8 cells in 2D (upper panels) and 3D (lower panel) cultures. E-cadherin and vimentin immunostaining of cell blocks from adherent PK-8 cells (upper panels) or PK-8 spheres (lower panel). Arrows indicate E-cadherin-positive cells. Scale bar in the phase contrast image of 2D culture: 200 μm , 3D culture: 100 μm ; SEM images in 2D culture: 20 μm , 3D culture: 50 μm ; immunocytochemistry: 50 μm .

cytoplasmic membrane of PK-8 cells, whereas no vimentin signal was detected under this 3D culture condition (Fig. 1, lower right panels). Observation of the cross-section of the PK-8 cell spheres also showed large and small cysts with circular to elliptical shapes (Fig. 1, lower right panels).

3.2. OCT observation of the spheres reveals internal cysts

Next, to examine the internal structure of the cyst of PK-8 cells in detail, serial cross-sections were observed by OCT. OCT technology

using near-infrared rays allows the non-destructive observation of 3D structural features undetectable via microscopy, such as cavities and gaps inside cells. Using OCT, round-to-oval cysts of various sizes were found inside the sphere, and some cysts were interconnected (Fig. 2, Supplemental Movie 1). The longest diameter of the sphere of PK-8 cells after 7 days in culture was $480.2 \pm 55.6 \mu\text{m}$ (mean \pm S.D.) under the Z slices of OCT images. The number of cysts on the maximum split surface of the spheres was 3 ± 1.2 (mean \pm S.D.), and the diameter of the cysts was $178.3 \pm 95.8 \mu\text{m}$ (mean \pm S.D.).

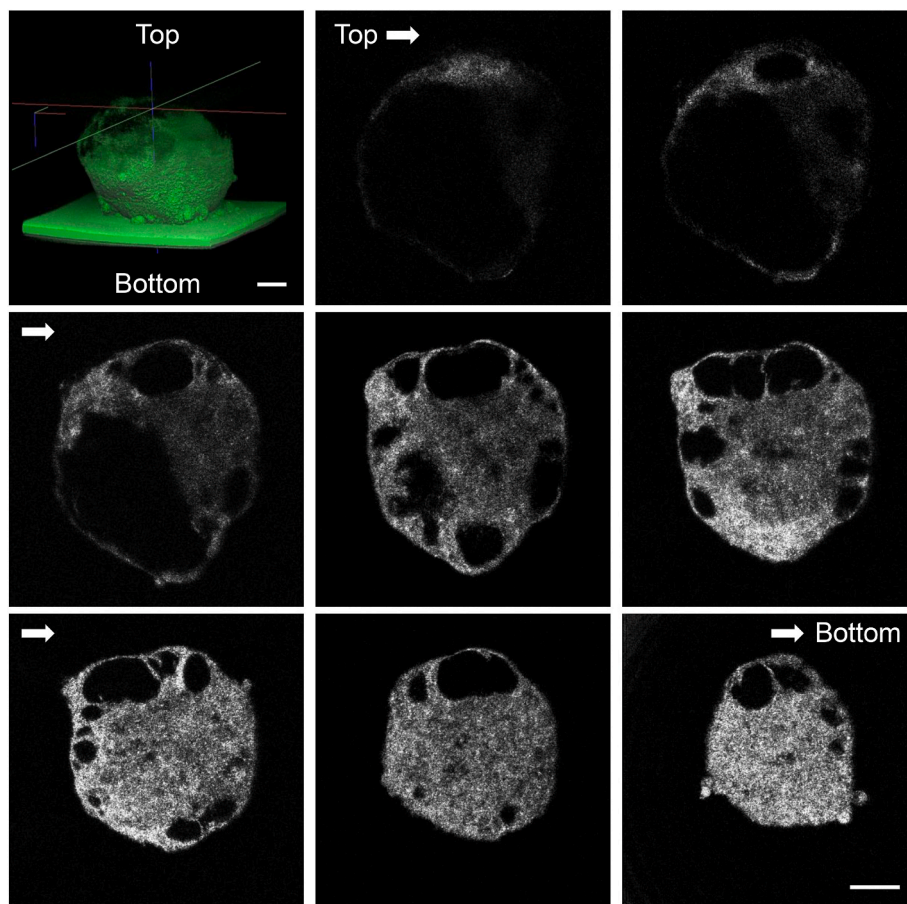


Fig. 2. Cross-sectional images of the PK-8 spheres using optical coherence tomography. Round to oval cysts of various sizes were observed in the spheres, and some cysts were interconnected. Scale bars: 100 μm .

3.3. TEM analysis of the PK-8 spheres

To examine the microstructure of the PK-8 spheres, TEM analysis was performed. The cyst wall consisted of a single layer of PK-8 cells with microvilli (Fig. 3A, arrowheads). The adhesion between the PK-8 cells in the spheres was weak, and a space between the cells was observed (Fig. 3A, asterisks). In the spheres, organelles and nuclei were degenerated in some PK-8 cells (Fig. 3B, arrow), and necrotic organelles were observed in other cells (Fig. 3C, arrow). Moreover, electron-dense circular secretory granules were detected in the cytoplasm of the PK-8 cells (Fig. 3D, arrows).

3.4. Dysregulation of fluid secretion-related molecules was detected in PK-8 spheres

To investigate whether PK-8 spheres increased fluid secretion, we performed qRT-PCR to examine the expression levels of endocrine and exocrine molecules and mucin. When compared with that in adherent cells, the mRNA level of *MUC1*, *MUC5AC*, and *AMY2A*, a pancreas-specific amylase, was significantly higher in the PK-8 spheres (Fig. 4A, $p < 0.05$). In contrast, no change in the expression of the genes coding for insulin and glucagon in the PK-8 spheres was detected as compared to adherent cells (Fig. 4A).

To confirm the high expression of *MUC1*, *MUC5AC*, and amylase at the protein level in the PK-8 spheres, immunocytochemical analysis was performed. Consistent with the mRNA expression levels, the number of cells positive for *MUC1*, *MUC5AC*, and amylase was increased in the spheres of PK-8 cells compared to that in adherent cells (Fig. 4B). The percentages of cells positive for *MUC1*, *MUC5AC*, and amylase are presented in Fig. 4C.

4. Discussion

Although PDAC cell lines possess different genetic mutations, they show a similar morphology under 2D culture. Recently, we identified two categories of PDAC cells based on their E-cadherin and vimentin expression levels [5,10]. Among the eight PDAC cell lines examined, PK-8 cells showed a 120,000 fold increase in E-cadherin mRNA expression when compared with the MIA PaCa-2 cells, which had the lowest E-cadherin level [9]. Epithelial-featured PDAC cell lines, with

high E-cadherin and low vimentin expression, form small, round spheres exhibiting a smooth surface and flat lining cells on their surface. On the other hand, mesenchymal-featured PDAC cell lines with opposite expression pattern form irregularly shaped spheres that contain small round to oval cancer cells and exhibit a grape-like appearance without flat lining cells [5,9,10]. Only PK-8 cells presented a large number of cystic and ductal structures in their spheres. It has been reported that ductal structures and basal lamina are formed under 3D culture when Matrigel is used together with well-differentiated PDAC cells but not with poorly differentiated PDAC cells [14]. We investigated whether the structure in the spheres of PK-8 cells was a duct. No basement membrane-like structures were observed by TEM analysis, and no laminin- or type 4 collagen-positive basement membrane-like structures were observed by immunocytochemical staining. PARD3 is a member of the apical membrane proteins, and immunocytochemical analysis revealed no PARD3 staining on the luminal side of cystic structures. These findings suggest that these structures are not pancreatic duct-like structures, but cysts formed between PK-8 cells in the spheres.

OCT images showed various sizes of cysts, some of which were connected to each other. TEM observations revealed loose binding between PK-8 cells throughout the sphere, with various stages of degenerated and necrotic PK-8 cells. Furthermore, many secretory granules were observed in some of the PK-8 cells that formed spheres. This evidence suggests that PK-8 cells synthesize and secrete substances that are stored in the cysts, and further individual cell degeneration and necrosis of PK-8 cells occur in the spheres. Due to the small size of the cyst and the small amount of fluid, we were unable to extract intracystic fluid for analysis. Therefore, we examined the PK-8 spheres for the expression of mucin and endocrine and exocrine molecules, which are mainly produced by pancreatic cells.

Mucus is commonly synthesized and secreted by normal ductal cells. Alcian-blue stains acidic mucus blue, whereas periodic acid-Schiff (PAS) staining turns neutral mucus red. Alcian blue staining was limited in 2D-cultured PDAC cell lines but abundant in some PDAC cell lines with epithelial features in 3D culture [9]. Similarly, PAS staining intensity in PDAC cell lines was stronger in spheres from 3D cultures than in those from 2D-cultured cells [9]. Mucin is a heavily glycosylated high-molecular-weight glycoprotein that is the main component of the mucus. In pancreatic tissue, the difference in staining patterns between MUC types is used for the differential diagnosis of PDAC and intraductal

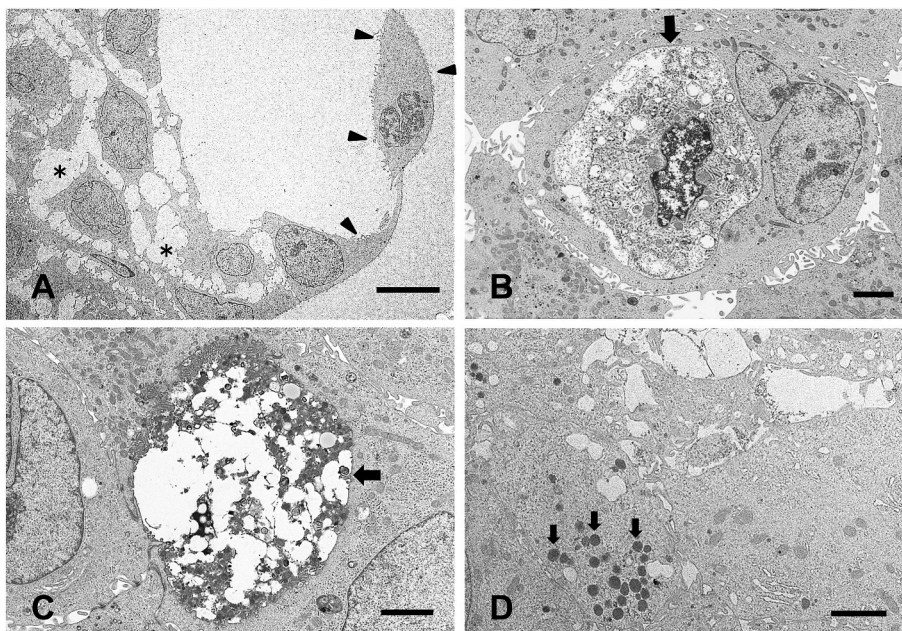


Fig. 3. Transmission electron microscopic analysis of PK-8 spheres.

The surface of the cyst is formed by a single layer of PK-8 cells (A, arrowheads), and the adhesion between PK-8 cells in the spheres is weak (A, asterisks). PK-8 cells that had undergone degeneration (B, arrow) and necrosis (C, arrow). A large number of secretory granules were observed in PK-8 cells (D, arrows). Scale bar in A:10 μm , B, C, and D:2 μm .

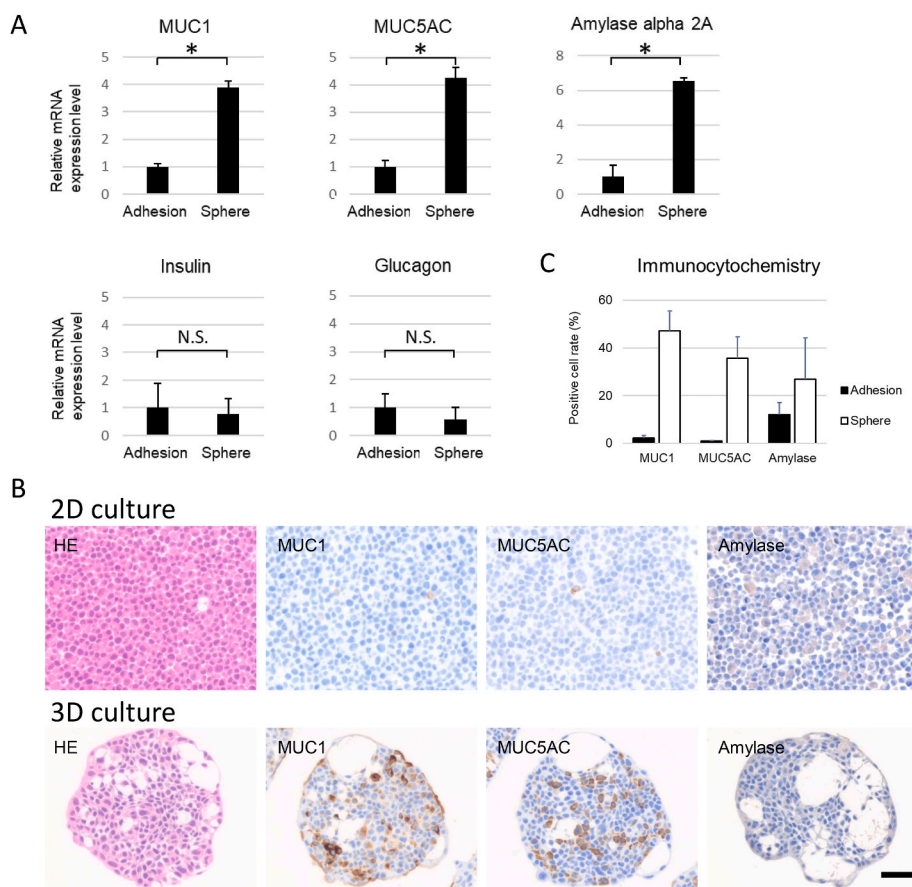


Fig. 4. Expression of mucin, exocrine, and endocrine molecules under 2D and 3D culture conditions. qRT-PCR analysis of pancreas-related molecules in PK-8 cells cultured under 2D (adhesion) and 3D conditions (spheres, A). Immunocytochemical analysis of MUC1, MUC5AC, and amylase alpha 2A in cell blocks from PK-8 cells cultured under 2D and 3D conditions (B). Scale bar for 2D and 3D culture: 50 μ m, * p < 0.05, N.S: not significant. Percentages of cells positive for MUC1, MUC5AC, and amylase alpha 2A in the adherent cells and spheres (C).

papillary mucinous neoplasms (IPMN). Most PDACs are positive for MUC1 and MUC5AC and negative for MUC2, whereas IPMN is positive for both MUC2 and MUC5AC and negative for MUC1 [15–17]. MUC1 is classified as a membrane-bound mucin, and MUC2 and MUC5AC are secreted mucins [18–20]. qRT-PCR and immunocytochemical analyses showed increased expression of MUC1 and MUC5AC in the PK-8 spheres. With regard to the exocrine components, amylase alpha 2A, a pancreas-specific amylase, increased in the spheres, whereas trypsin was below the detection levels in both 2D and 3D culture. No change in the endocrine components at the mRNA level was detected in the PK-8 spheres as compared with that in the adherent cells.

These findings suggest that MUC1, MUC5AC, and amylase are synthesized more in the PK-8 spheres than in 2D-culture, and these components are part of the contents of cysts. Electron microscopic secretory granules in PK-8 spheres may correlate with an increase in amylase synthesis. The current study could not directly demonstrate the ability of mucins or amylases to form cysts. However, based on our examination of cell blocks of PK-8 spheres, in which cells in the center of the spheres produced amylase, an exocrine molecule, and MUC5AC, a secreted mucin, and based on the observation that the surface of the spheres was covered by flat lining cells, we believe that these molecules may accumulate between cancer cells in the spheres and form cysts. Decreasing the expression levels of mucins or amylase in PK-8 cells using shRNA or siRNA may clarify the importance of these molecules in multiple cyst formation in the spheres. The biological significance or contribution of cyst-forming 3D-cultured PDAC cells to the development of diagnostic or therapeutic methods is not clear. Further studies are needed to clarify the clinical importance of cyst-forming PDAC cells.

In summary, PK-8 cells, as PDAC cells highly expressing E-cadherin, formed spheres with multiple cysts. The connections between the PK-8 cells forming the sphere were loose, and individual cell degeneration and necrosis were observed. Although the fluid in the cyst could not be

examined because of its small amount, the PK-8 cells forming the sphere showed secretory granules and an increase in mucins and exocrine fluid. These findings suggest that increased mucin and amylase synthesis contributes to the PK-8 cells' ability to form multiple cystic spheres.

Funding

This work was supported by JSPS KAKENHI Grant Numbers 21K08744, 21K08764, and 22K08882 (Grant-in-Aid for Scientific Research C).

Authors contribution

Conception and design of the study: Y. S., F.G and T.I. Acquisition and interpretation of data: Y.S., F.G., Y.U., F.H., Y.H., K.N., H.Y., M.Y., K. T., T.A., and T.I. Drafting the article: Y.S. and T.I. Revising the manuscript critically for important intellectual content: K.N., N.H., H.Y., M.Y., K.T., and T.A.

Declaration of competing interest

The authors have declared that no conflict of interest exists.

Acknowledgements

The authors thank Ms. Masako Kida and Mr. Yasushi Kuromi (SCREEN Holdings Co., Ltd.) for their technical assistance with OCT photography.

Appendix A. Supplementary data

Supplementary data to this article can be found online at <https://doi.org/10.1016/j.bbrep.2022.101339>.

org/10.1016/j.bbrep.2022.101339.

References

- [1] P. Rawla, T. Sunkara, V. Gaduputi, Epidemiology of pancreatic cancer: global trends, etiology and risk factors, *World J. Oncol.* 10 (2019) 10–27, <https://doi.org/10.14740/wjon1166>.
- [2] J. He, N. Ahuja, M.A. Makary, J.L. Cameron, F.E. Eckhauser, M.A. Choti, R. H. Hruban, T.M. Pawlik, C.L. Wolfgang, 2564 resected periampullary adenocarcinomas at a single institution: trends over three decades, *HPB* 16 (2014) 83–90, <https://doi.org/10.1111/hpb.12078>.
- [3] J. Kleeff, M. Korc, M. Apte, C. La Vecchia, C.D. Johnson, A.V. Biankin, R.E. Neale, M. Tempero, D.A. Tuveson, R.H. Hruban, J.P. Neoptolemos, Pancreatic cancer, *Nat. Rev. Dis. Prim.* 2 (2016), 16022, <https://doi.org/10.1038/nrdp.2016.22>.
- [4] L. Rahib, B.D. Smith, R. Aizenberg, A.B. Rosenzweig, J.M. Fleshman, L. M. Matrisian, Projecting cancer incidence and deaths to 2030: the unexpected burden of thyroid, liver, and pancreas cancers in the United States, *Cancer Res.* 74 (2014) 2913–2921, <https://doi.org/10.1158/0008-5472.CAN-14-0155>.
- [5] Y. Shichi, F. Gomi, N. Sasaki, K. Nonaka, T. Arai, T. Ishiwata, Epithelial and mesenchymal features of pancreatic ductal adenocarcinoma cell lines in two- and three-dimensional cultures, *J. Personalized Med.* 12 (2022), <https://doi.org/10.3390/jpm12050746>.
- [6] K.M. Yamada, E. Cukierman, Modeling tissue morphogenesis and cancer in 3D, *Cell* 130 (2007) 601–610, <https://doi.org/10.1016/j.cell.2007.08.006>.
- [7] E. Vincan, T. Brabletz, M.C. Faux, R.G. Ramsay, A human three-dimensional cell line model allows the study of dynamic and reversible epithelial-mesenchymal and mesenchymal-epithelial transition that underpins colorectal carcinogenesis, *Cells Tissues Organs* 185 (2007) 20–28, <https://doi.org/10.1159/000101299>.
- [8] E.A. Collisson, A. Sadanandam, P. Olson, W.J. Gibb, M. Truitt, S. Gu, J. Cooc, J. Weinkle, G.E. Kim, L. Jakkula, H.S. Feiler, A.H. Ko, A.B. Olshen, K.L. Danenberg, M.A. Tempero, P.T. Spellman, D. Hanahan, J.W. Gray, Subtypes of pancreatic ductal adenocarcinoma and their differing responses to therapy, *Nat. Med.* 17 (2011) 500–503, <https://doi.org/10.1038/nm.2344>.
- [9] F. Minami, N. Sasaki, Y. Shichi, F. Gomi, M. Michishita, K. Ohkusu-Tsukada, M. Toyoda, K. Takahashi, T. Ishiwata, Morphofunctional analysis of human pancreatic cancer cell lines in 2- and 3-dimensional cultures, *Sci. Rep.* 11 (2021) 6775, <https://doi.org/10.1038/s41598-021-86028-1>.
- [10] Y. Shichi, N. Sasaki, M. Michishita, F. Hasegawa, Y. Matsuda, T. Arai, F. Gomi, J. Aida, K. Takubo, M. Toyoda, H. Yoshimura, K. Takahashi, T. Ishiwata, Enhanced morphological and functional differences of pancreatic cancer with epithelial or mesenchymal characteristics in 3D culture, *Sci. Rep.* 9 (2019), 10871, <https://doi.org/10.1038/s41598-019-47416-w>.
- [11] T. Yamaguchi, S. Ikehara, Y. Akimoto, H. Nakanishi, M. Kume, K. Yamamoto, O. Ohara, Y. Ikehara, TGF-beta signaling promotes tube-structure-forming growth in pancreatic duct adenocarcinoma, *Sci. Rep.* 9 (2019), 11247, <https://doi.org/10.1038/s41598-019-47101-y>.
- [12] F. Gomi, N. Sasaki, Y. Shichi, F. Minami, S. Shinji, M. Toyoda, T. Ishiwata, Polyvinyl alcohol increased growth, migration, invasion, and sphere size in the PK-8 pancreatic ductal adenocarcinoma cell line, *Heliyon* 7 (2021), e06182, <https://doi.org/10.1016/j.heliyon.2021.e06182>.
- [13] T. Ishiwata, F. Hasegawa, M. Michishita, N. Sasaki, N. Ishikawa, K. Takubo, Y. Matsuda, T. Arai, J. Aida, Electron microscopic analysis of different cell types in human pancreatic cancer spheres, *Oncol. Lett.* 15 (2018) 2485–2490, <https://doi.org/10.3892/ol.2017.7554>.
- [14] H. Yamanari, T. Suganuma, T. Iwamura, N. Kitamura, S. Taniguchi, T. Setoguchi, Extracellular matrix components regulating glandular differentiation and the formation of basal lamina of a human pancreatic cancer cell line in vitro, *Exp. Cell Res.* 211 (1994) 175–182, <https://doi.org/10.1006/excr.1994.1075>.
- [15] J. Lüttges, G. Zamboni, D. Longnecker, G. Klöppel, The immunohistochemical mucin expression pattern distinguishes different types of intraductal papillary mucinous neoplasms of the pancreas and determines their relationship to mucinous noncystic carcinoma and ductal adenocarcinoma, *Am. J. Surg. Pathol.* 25 (2001) 942–948, <https://doi.org/10.1097/00000478-200107000-00014>.
- [16] G.E. Kim, H.I. Bae, H.U. Park, S.F. Kuan, S.C. Crawley, J.J. Ho, Y.S. Kim, Aberrant expression of MUC5AC and MUC6 gastric mucins and sialyl TN antigen in intraepithelial neoplasms of the pancreas, *Gastroenterology* 123 (2002) 1052–1060, <https://doi.org/10.1053/gast.2002.36018>.
- [17] A. Nakamura, M. Horinouchi, M. Goto, K. Nagata, K. Sakoda, S. Takao, K. Imai, Y. S. Kim, E. Sato, S. Yonezawa, New classification of pancreatic intraductal papillary-mucinous tumour by mucin expression: its relationship with potential for malignancy, *J. Pathol.* 197 (2002) 201–210, <https://doi.org/10.1002/path.1109>.
- [18] M.A. Hollingsworth, B.J. Swanson, Mucins in cancer: protection and control of the cell surface, *Nat. Rev. Cancer* 4 (2004) 45–60, <https://doi.org/10.1038/nrc1251>.
- [19] Y. Itoh, M. Kamata-Sakurai, K. Denda-Nagai, S. Nagai, M. Tsujii, K. Ishii-Schrade, K. Okada, A. Goto, M. Fukayama, T. Irimura, Identification and expression of human epiglycanin/MUC21: a novel transmembrane mucin, *Glycobiology* 18 (2008) 74–83, <https://doi.org/10.1093/glycob/cwm118>.
- [20] N. Moniaux, F. Escande, N. Porchet, J.P. Aubert, S.K. Batra, Structural organization and classification of the human mucin genes, *Front. Biosci.* 6 (2001) D1192–D1206, <https://doi.org/10.2741/moniaux>.